7. J. M. Ortega and W. C. Reinboldt, Iterative Solution of Nonlinear Equations in Several Variables, Academic Press (1970).
8. G. A. Korn and T. M. Korn, Manual of Mathematics, McGraw-Hill (1967).
9. A. G. Bondarenko, I. F. Golubev, and I. M. Britan, Teor. Osn. Khim. Tekhnol., 17, No. 1, 106-108 (1983).
10. N. A. Kolokol'tsov, N. I. Laguntsov, and G. A. Sulaberidze, At. Energ., 34, No. 4, 259-263 (1973).
11. V. D. Borisevich, V. K. Ezhov, V. Yu. Kozhevnikov et al., Teor. Osn. Khim. Tekhnol., 17, No. 2, 172-177 (1983).
12. E. B. Gruzdev, N. K. Laguntsov, B. I. Nikolaev et al., At. Energ., 57, No. 2, 117-120 (1984).
13. N. I. Nikolaev, Diffusion in Membranes [in Russian], Moscow (1980).
14. V. D. Borisevich, N. N. Grishaev, N. I. Laguntsov, and G. A. Sulaberidze, Teor. Osn. Khim. Tekhnol., 18, No. 1, 20-24 (1984).

HEAT AND MASS TRANSFER IN THE STEADY WALL COMBUSTION OF A FILTRATED GAS MIXTURE

G. T. Sergeev

UDC 536.46

The influence of external and internal heat and mass transfer on the temperature distribution in the solid and gas phases and on the stability of the combustion zone in "standing-wave" conditions is investigated.

Surface combustion of filtrated fuel, which occurs in porous radiators, refractory preheaters, and chemical-technology processes and apparatus, is a complex phenomenon whose analysis entails taking account of heat and mass transfer of interacting media and the chemical kinetics of homogeneous reaction of the components. In [1, 2], where surface combustion was investigated for a porous radiator, it was assumed that the temperatures of the body skeleton $t_T = (T_T - T_\infty)/T_\infty$ and the filtrated fuel $t_I = (T_I - T_\infty)/T$ are the same.

In the present work, the results of theoretical investigation of the surface combustion of filtrated fuel are given, together with an analysis of the conditions corresponding to a "standing wave," taking account of the difference in t_T and t_I. The results of analytical investigations are compared with experiment.

The problem is formulated as follows. A stoichiometric gas mixture is filtered through a semiinfinite body (Fig. 1), consisting of a chemically inert porous medium ($-\infty \leq x \leq 0$) with impermeable heat-insulated side walls, at a velocity $v = (j/\rho)_I$, where j_I is the total density of a longitudinal flux of injectant consisting of fuel j_f and oxidant j_o ($j_I = j_f + j_o$); ρ_I is the gravimetric density of the gas mixture. It is assumed that the chemical reaction of the porous medium with the injected gas does not occur; the thermophysical properties of the interacting media and the porosity of the medium do not change in the course of the process; the rate of chemical combustion is infinitely large in comparison with the diffusion rate, i.e., the flame-front model is valid; filtrational effects may be neglected. The latter assumption, allowing the filtration equation to be eliminated from consideration, does not lead to significant calculation errors, since the present work is an investigation of conditions of low injection rate of injectant relative to a porous radiator with surface combustion, for which $v_\infty = 0.37$-0.172 m/sec [1, 2], at large filtration coefficients and porosity of the body skeleton $\Pi = 80\%$.

The following physical picture is considered. Combustion of the injectant is initiated by a source (acting only at the initial moment of time) at the end surface of the body ($x = 0$).

A. V. Lykov Institute of Heat and Mass Transfer, Minsk. Translated from Inzhenerno-Fizicheskii Zhurnal, Vol. 51, No. 6, pp. 924-931, December, 1986. Original article submitted October 2, 1985.

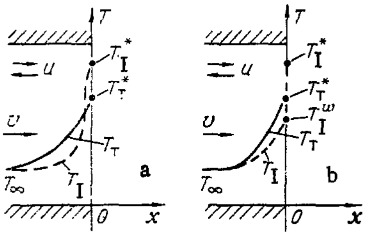

Fig. 1

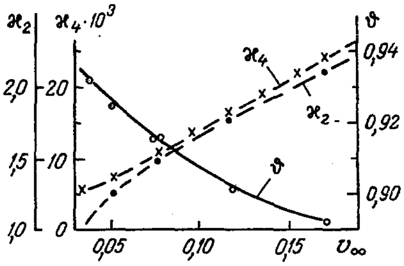

Fig. 2

Fig. 1. Temperature distribution in porous body: T_T, for solid; T_I, for gas mixture; v is the injection rate of the injectant and u is the velocity of the combustion wave.

Fig. 2. Dependence of the roots κ_2, κ_4, and $\vartheta = t_T^*/t_I^*$ on v_∞ (m/sec).

In the course of the whole process, combustion occurs in the region x = 0 (in the wall gas layer and in pores of the body), which is the heat-liberation zone, where $T_I^* > T_T^*$ (Fig. 1). The high-temperature combustion products which form here heat the porous packing. In the heating zone (x < 0), where $T_T > T_I$, the packing loses heat to the gas. In addition, in the cooling zone (x > 0), convective heat transfer of the packing surface with the surrounding medium occurs. Hence, in the steady process in the combustion zone, $T_I^* > T_T^*$. This two-temperature model is confirmed by experimental investigations of filtrational combustion of hydrogen-air mixtures [3].

In analyzing filtrational combustion, mobile $\bar{X}$, $\bar{\tau}$ and immobile X, τ coordinate systems relative to a combustion wave moving at velocity u are used below: $X = \bar{X} - \mathrm{Pe}_I \mathrm{Fo}$, $X = x/l_E$, $\bar{X} = \bar{x}/l_E$, $\tau = \bar{\tau}$, where x and $\bar{x}$ are the abscissas; τ and $\bar{\tau}$ are time; l_E is an equivalent dimension equal to the ratio of inertial β_1 (m^{-1}) and hydraulic β_2 (m^{-2}) drag coefficients ($l_E = \beta_1/\beta_2$); $\mathrm{Pe}_I = u l_E/a_T$ is the Peclet number; $\mathrm{Fo} = a_T \tau / l_E^2$ is the Fourier number. The air direction v is taken as the positive direction of the combustion-wave velocity u.

The differential equations for the temperatures of the body skeleton and the injectant are written in the following form [4]

$$\frac{\partial t_T}{\partial \mathrm{Fo}} = \frac{\partial^2 t_T}{\partial X^2} + \mathrm{Pe}_I \frac{\partial t_T}{\partial X} + \mathrm{Nu}_V (t_I - t_T),$$
$$\varkappa \frac{\partial t_I}{\partial \mathrm{Fo}} = \frac{\partial^2 t_I}{\partial X^2} - \mathrm{Pe}_\Delta \frac{\partial t_I}{\partial X} - \chi \mathrm{Nu}_V (t_I - t_T) + \mathrm{Ki}_\delta. \tag{1}$$

Analytical expressions for the dimensionless parameters χ and Ki_δ, which appear in Eq. (1) and which characterize the thermal inertia of the system and the heat liberation at the surface of the permeable body on account of the combusion, respectively, and also for the Nusselt number Nu_V and Peclet number Pe_Δ, which depend on the internal heat transfer and the injection rate of the gas and the velocity of combustion-front motion, take the form

$$\chi = \frac{(1-\Pi)\lambda_T}{\Pi \lambda_I}, \quad \mathrm{Ki}_\delta = \frac{Q j \eta_b l_E^2}{\lambda_I T_\infty} \delta(X-0),$$
$$\varepsilon = \frac{a_T}{a_I}, \quad \mathrm{Pe}_\Delta = \frac{(v_\infty - u) l_E}{a_I},$$
$$\mathrm{Nu}_V = \frac{\alpha_V l_E^2}{a_T}, \quad \alpha_V = \frac{\alpha}{(1-\Pi) c_{pT} \rho_T}, \tag{2}$$

where δ(X — 0) is a Dirac delta function equal to infinity when X = 0 and zero when X ≠ 0, characterizing the heat liberation on account of combustion; Q is the thermal effect of the reaction; η_b is a coefficient characterizing the completeness of burnup of the injectant; α ($J/m^3 \cdot sec \cdot K$) is the internal heat-transfer coefficient between the body skeleton and the injectant, determined by the relation [5]: $\mathrm{Nu} = 0.515 \cdot \mathrm{Re}^{0.85} \mathrm{Pr}^{0.33}$ ($\mathrm{Nu} = \alpha l_E^2/\lambda_I^*$, $\mathrm{Re} = j l_E/\mu_I^*$).

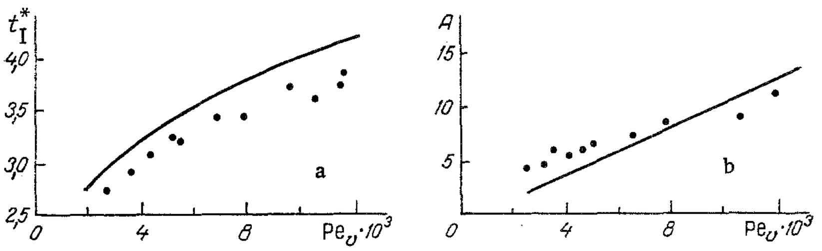

Fig. 3. Dependence of the injectant temperature t_I^* at X = 0 and the parameter A characterizing the "standing wave" on the Peclet number Pe_v; the curves correspond to theory and the points to experiment.

Realization of the flame-front model with an infinitely thin reaction zone allows a δ source to be introduced into Eq. (1) for t_I, and hence the solution of the problem may be obtained in finite form.

Investigating the heat and mass transfer in the surface combustion of a filtrated mixture reduces, in the given case, to analyzing the problem of steady propagation of the reaction zone, i.e., to solving Eq. (1) with $\partial t_T/\partial Fo = \partial t_I/Fo = 0$ and the following boundary conditions

$$X=0,\ t_I=t_I^*,\ t_T=t_T^*, \tag{3}$$

$$\frac{\partial t_I}{\partial X}+Bi_I^w t_I^* = Ki^*,\ \ \frac{\partial t_T}{\partial X}+Bi_T^w t_T^* = Ki^*, \tag{4}$$

$$X=-\infty,\ t_T=t_I=0, \tag{5}$$

where $Bi_I^w = \bar{\alpha}^w l_E/\lambda_I$, $Bi_T^w = \bar{\alpha}^w l_E/\lambda_T$ are the Biot number determining the heat transfer at x = 0; the dimensionless parameter $Ki^* = Q j_b \eta_b l_E / T_\infty \lambda_I$ characterizes the energy source due to combustion of the gas mixture of fuel with oxidant. The first and second terms on the left-hand side in Eq. (4) are the conductive and convective components of the heat flux. The conditions in Eqs. (3) and (5) determine the temperature at the body surface and at infinity in the body. The heat-transfer coefficient of the surface of the permeable body with the surrounding medium $\bar{\alpha}^w$ appearing in the numbers Bi_T^w and Bi_I^w is determined by a relation corresponding to the experimental conditions of [2].

$$\bar{\alpha}^w = \frac{\lambda_I}{L} Nu_e + \frac{1}{t_I^*}\left(j_I H + q_R - \lambda_\Sigma \nabla T_\Sigma + P_I \sum_j^N k_j^T V_j + \sum_j^N h_j \rho_j V_j\right). \tag{6}$$

The first term on the right-hand side here is due to natural convection, the second to gas injection, the third to radiation of the wall and gases, the fourth to conduction, and the fifth to diffusion of molecules in the coordinate system moving at the hydrodynamic (mean-mass) velocity $V_j (V_j = j_j/\rho_j)$; L is the characteristic dimension (the thickness of the gas layer above a horizontal radiating screen); H is the enthalpy of the gas mixture; h_j is the enthalpy of the j-th gas component in the N-component mixture. For Nusselt number Nu_e and the component q_R, the following expressions may be written

$$Nu_e = c(Gr\,Pr)^n,\ \ q_R = q_w + q_{cd} + q_v, \tag{7}$$

where the constants c and n are functions of the product GrPr, which varies in the range 210-115,000; the term q_w is due to the radiation of the screen (permeable surface), q_{cd} to that of carbon dioxide CO_2, and q_v to that of water vapor H_2O.

Calculations by Eqs. (6) and (7) are simplified in that the composition of the combustion products of the injectant corresponds sufficiently accurately to a mixture of dusty gases [1, 2]. The method of calculating the terms in Eqs. (6) and (7) and the experimental method were described in more detail in [6].

In the given case — steady propagation of a combustion wave — it follows from the continuity equation that [3, 4]

$$\rho_I(v-u) = \rho_{I\infty}(v_\infty - u).$$

Equation (1) is linear for the zone $-\infty \leq X \leq 0$, in which the concentration of the deficient component (the fuel) is $Y_I = Y_{I\infty}$. In the combustion zone, where $X = 0$, $Y_I = 0$. The eigenvalues κ_i, $i = 1, 2, 3, 4$ of Eq. (1) are determined by solving the characteristic equation

$$\varkappa^4+(\mathrm{Pe}_I-\mathrm{Pe}_\Delta)\varkappa^3-[\mathrm{Nu}_V(1+\chi)+\mathrm{Pe}_I\mathrm{Pe}_\Delta]\varkappa^2+\mathrm{Nu}_V(\mathrm{Pe}_\Delta-\chi\mathrm{Pe}_I)\varkappa=0. \tag{8}$$

It follows from analysis of Eq. (8) that, for small flame-front velocities and large thermal inertia of the solid phase, i.e., when

$$u\ll v,\ \chi\gg 1, \tag{9}$$

the roots κ_i are real (Fig. 2): $\kappa_1 = 0$, $\kappa_2 > \kappa_4 > 0$, $\kappa_3 < 0$; the solution of Eqs. (1)-(5) for the region $X \leq 0$ is determined solely by the eigenvalues κ_1, κ_2, and κ_4; in Eq. (9) and below, $v = v_\infty$. The roots κ_i, $i = 2, 3, 4$ corresponding to the parameters of Eqs. (19) and (20) below vary in the range (Fig. 2): $\kappa_2 = 0.5\text{-}2.7$; $\kappa_3 = -(0.4\text{-}2.5)$, $\kappa_4 = (3\text{-}30)\cdot 10^{-3}$.

As a result of solving Eq. (1), and taking account of the boundary conditions in Eqs. (3) and (5) and also Eq. (9), it is found that

$$\begin{aligned} t_I&=[\gamma_2(t_I^*+\gamma_4 t_T^*)\exp\varkappa_2X-\gamma_4(t_I^*+\gamma_2t_T^*)\exp\varkappa_4X](\gamma_2-\gamma_4)^{-1},\\ t_T&=[(t_I^*+\gamma_2t_T^*)\exp\varkappa_4X-(t_I^*+\gamma_4t_T^*)\exp\varkappa_2X](\gamma_2-\gamma_4)^{-1}, \end{aligned} \tag{10}$$

where

$$\gamma_i=\frac{\varkappa_i}{\mathrm{Nu}_V}(\varkappa_i+\mathrm{Pe}_I)-1,\ i=2, 4.$$

From the boundary conditions in Eq. (4), using the solution in Eq. (10), the following theoretical dependences are obtained for the dimensionless temperature of the gas t_I^* and the body of the skeleton t_T^* at the surface of the body coinciding with the combustion zone

$$\begin{aligned} t_I^*&=\mathrm{Ki}^*[(\varkappa_4\gamma_2-\varkappa_2\gamma_4)-\tilde\lambda^{-1}\gamma_2\gamma_4(\varkappa_2-\varkappa_4)+\mathrm{Bi}_T^w(\gamma_2-\gamma_4)]w^{-1},\\ t_T^*&=\mathrm{Ki}^*[\tilde\lambda(\varkappa_2\gamma_2-\varkappa_4\gamma_4)+(\varkappa_2-\varkappa_2)+\mathrm{Bi}_T^w(\gamma_2-\gamma_4)]w^{-1}, \end{aligned} \tag{11}$$

where

$$w=(\gamma_2-\gamma_4)(\mathrm{Bi}_I^w\mathrm{Bi}_T^w+\varkappa_2\varkappa_4)+\mathrm{Bi}_T^w[(\varkappa_2\gamma_2-\varkappa_4\gamma_4)+\tilde\lambda(\varkappa_4\gamma_2-\varkappa_2\gamma_4)],\ \tilde\lambda=\lambda_T/\lambda_I.$$

The solution in Eqs. (10) and (11) of the problem in Eqs. (1)-(5) allows the temperature values at the surface of the permeable body and their distribution in the solid and gas phases to be determined sufficiently accurately. Theoretical curves of $\vartheta=\vartheta(v_\infty)$, where $\vartheta=t_T^*/t_I^*$, are shown in Fig. 2, and comparison of theory with experiment for t_I^* in Fig. 3a. For the given conditions, the parameter ϑ varies in the limits 0.89-0.93; the maximum difference in the theoretical and experimental values of t_I^* (for the whole range of Pe_V) is no greater than ±20%.

The Peclet number Pe_I is found from Eqs. (1)-(5). Integrating the first relation in Eq. (1) over the limits from 0 to $-\infty$, and taking account of the second boundary condition in Eq. (4), a dependence is obtained for qualitative analysis of the dimensionless combustion-wave velocity Pe_I

$$\mathrm{Pe}_I=\varepsilon(\mathrm{Bi}_T^w-\eta), \tag{12}$$

where

$$\eta=(\mathrm{Ki}^*\tilde\lambda^{-1}-z\mathrm{Nu}_V)/t_T^*;\ z=J/L_E T_\infty;\ J=\int_{-\infty}^{0}(t_T-t_I)dx>0.$$

The number $\mathrm{Pe}_I = 0$ when

$$\mathrm{Bi}_T^w t_T^*=\tilde\lambda^{-1}\mathrm{Ki}^*-z\mathrm{Nu}_V, \tag{13}$$

$\mathrm{Pe}_I > 0$ when $\mathrm{Bi}_T^w > \eta$, and $\mathrm{Pe}_I < 0$ when $\mathrm{Bi}_T^w < \eta$.

According to Eq. (8), determining the combustion-wave velocity in the general case entails solving an equation of fourth order in u or Pe_I. However, this analysis is possible if the temperature values of the solid and gas phases are known at the combustion surface.

Below, with the aim of simplifying the dependences for calculating the combustion-wave velocities, it is assumed that, according to [6], convective heat transfer dominates in the gas phase, and therefore, the conductive term ($\partial^2 t_I/\partial X^2 = 0$) in Eq. (1) may be neglected.

When $t_I'' = 0$, the eigenvalues $\bar{\kappa}_i$ of the linear steady system in Eq. (1) are determined by the characteristic equation

$$\bar{\varkappa}^2+\bar{\varkappa}\psi-\mathrm{Nu}_V(1-\chi\mathrm{Pe}_I/\mathrm{Pe}_\Delta)=0,$$

where

$$\bar{\varkappa}_{1,2}=-\frac{\psi}{2}\pm\sqrt{\frac{\psi^2}{4}+\mathrm{Nu}_V\left(1-\chi\frac{\mathrm{Pe}_I}{\mathrm{Pe}_\Delta}\right)};\quad \psi=\mathrm{Pe}_I+\frac{\chi\mathrm{Nu}_V}{\mathrm{Pe}_\Delta}, \tag{14}$$

and $\bar{\kappa}_1 > 0$, $\bar{\kappa}_2 < 0$.

The solution of Eqs. (1)-(5) in the region $X \leq 0$ when $t_I'' = 0$, taking account of Eq. (9) is determined solely by eigenvalue $\bar{\kappa}_1$. When Eqs. (3) and (5) are satisfied, it takes the form

$$t_T=t_T^*\exp\varkappa_1 X,\ t_I=\mathrm{Pe}_\Delta^{-1}[\mathrm{Ki}^*E(X-0)+\chi t_T^*(\varkappa_1+\mathrm{Pe}_I)]\exp\varkappa_1 X, \tag{15}$$

where E(X — 0) is the unit Heaviside function,

$$E(X-0)=\begin{cases}1, & X=0;\\ 0, & X\neq 0.\end{cases}$$

The temperature values at their discontinuity surfaces may be obtained from the second relation in Eq. (15)

$$t_I^w=\chi t_T^*(\varkappa_1+\mathrm{Pe}_I)\mathrm{Pe}_\Delta^{-1},\ t_I^*=[\mathrm{Ki}^*+\chi t_T^*(\bar{\varkappa}_1+\mathrm{Pe}_I)]\mathrm{Pe}_\Delta^{-1}. \tag{16}$$

As follows from the above analysis, Eqs. (10) and (11) correspond to continuous values of t_I and t_T (Fig. 1a); when using Eqs. (15) and (16), it is found that the gas temperature undergoes a discontinuity at X = 0 (Fig. 1b), i.e., to the left and right of the surface of the permeable body the values of T_I are T_I^W and T_I^*, respectively. In both cases, the values of T_T^* qualitatively agree.

It follows from an analysis of Eqs. (10) and (15) that the temperatures of the body skeleton and the injectant increase with decrease in injection rate Pe_v or v, thermal conductivity λ_I and λ_T, internal heat transfer Nu_V, or heat transfer with the surfaces of the body Bi_T^W and Bi_I^W and also with increase in heat of combustion Ki* and specific heats c_{pI} and c_{pT}. The difference in t_T and t_I increases on approaching the combustion surface.

From the second boundary condition in Eq. (4), using Eq. (15), a dependence is obtained for calculating Pe_I in the vicinity of the point X = 0

$$\mathrm{Pe}_I=\frac{-\mathrm{Ki}^*+t_I^*\mathrm{Pe}_v-\chi t_T^*\mathrm{Bi}_T^w}{t_I^*\varepsilon+t_T^*\chi}, \tag{17}$$

where $Pe_v = v l_E/a_I$; the temperatures t_I^* and t_T^* may be determined from Eq. (11), obtained on taking account of the conductive component in Eq. (1), i.e., when $\partial^2 t_I/\partial X^2 = 0$.

According to Eq. (17), the waves are cotraveling or opposed, respectively, when

$$t_I^*\mathrm{Pe}_v>\mathrm{Ki}^*+\chi t_T^*\mathrm{Bi}_T^w,\ t_I^*\mathrm{Pe}_v<\mathrm{Ki}^*+\chi t_T^*\mathrm{Bi}_T^w.$$

If the temperature of the body skeleton and the injectant in the combustion zone are equal $t_I^* = t_T^* = t^*$, Eq. (17) takes the form

$$\mathrm{Pe}_I=\frac{-\mathrm{Ki}^*/t^*+\mathrm{Pe}_v-\chi\mathrm{Bi}_T^w}{\varepsilon+\chi}. \tag{17a}$$

As follows from Eq. (17), the standing-wave stage ($Pe_I = u = 0$) is realized when

$$A=\mathrm{Pe}_v,\ A=(\mathrm{Ki}^*+\chi t_T^*\mathrm{Bi}_T^w)/t_I^*. \tag{18}$$

If $t_T^* = t_I^* = t^*$, Eq. (18) is written in the form

$$\mathrm{Ki}^*/t^* + \chi \mathrm{Bi}_T^w = \mathrm{Pe}_v. \tag{18a}$$

Thus, Eqs. (10), (11), and (15) allow the temperature values in the solid and gas phases to be determined, while Eqs. (17) and (17a) allow the velocity of the maximum-temperature zone (flame front) to be determined. Equations (18) and (18a) determine the position of the "standing wave." As already noted, according to the formulation of the problem in Eqs. (1)-(5), the conditions in which the combustion front initiated at the surface of the permeable body remains there throughout the whole process are considered.

A comparison of values of A and t_I^* obtained from Eqs. (11) and (18) and experimentally is given in Fig. 3. Note that Eq. (18), characterizing the "standing-wave" state, while relatively simple, allows the conditions corresponding to $\mathrm{Pe}_I = u = 0$ to be determined sufficiently accurately (Fig. 3b).

Calculations using Eqs. (10)-(18) are based on the following parameter values (at a determining temperature $T_0 = T_\infty$), corresponding to the combustion of methane—air mixture at the surface of ultralightweight chammotte [1, 2, 4]

$$\begin{gathered}\lambda_I = 0{,}024,\ \lambda_T = 0{,}73 \quad \mathrm{W/(m \cdot K)};\ \Pi = 0{,}8;\ c_{FI} = 979,\ c_{pT} = 148 \quad \mathrm{J/(kg \cdot K)};\\ \rho_I = 1{,}15,\ \rho_T = 3750\ \mathrm{kg/m^3};\ T_{T\infty} = T_{I\infty} = 293\ \mathrm{K};\ \chi = 7{,}7;\ a_I = 2{,}1 \cdot 10^{-5},\\ a_T = 1{,}315 \cdot 10^{-6}\ \mathrm{m^2/sec};\ l_E = 25 \cdot 10^{-6}\ \mathrm{m};\ Q = 51 \cdot 10^6 \quad \mathrm{J/kg},\ L = 0{,}024\ \mathrm{m}.\end{gathered} \tag{19}$$

The parameters in Eq. (19) correspond to experimental conditions of stable operation of porous radiators with surface combustion, in the absence of flame displacement (breakthrough or breakaway). Therefore, questions of flame motion, investigated in more detail in [7], are of independent scientific interest; they have not previously been considered. The experimental method was considered in more detail in [1, 2]. The experiments are conducted with combustion of a stoichiometric mixture of methane and air at the surface of a lightweight refractory and heating of metallic components by a radiator. Heat transfer (basically radiational) between the part and the radiator increases the error of calculation by Eqs. (10), (11), and (15), i.e., the difference between theory and experiment, since in solving Eqs. (1)-(5) no account is taken of the time-varying energy source due to the presence of the heated part.

The dimensionless parameters used in Eqs. (10)-(18) vary over the following limits, corresponding to Eq. (19) and experiment [1, 2, 4]

$$\begin{gathered}\mathrm{Pe}_v = (0{,}5\text{--}14) \cdot 10^{-3};\ \mathrm{Pe}_\Delta = (2{,}3\text{—}24) \cdot 10^{-2};\ t_I^* = 2{,}2\text{—}2{,}7;\\ \mathrm{Nu} = (15 \div 57) \cdot 10^{-3};\ \mathrm{Nu}_V = 0{,}1 \div 0{,}5;\ \mathrm{Bi}_T^w = (9\text{—}18) \cdot 10^{-2};\\ \mathrm{Bi}_I^w = (2\text{—}7) \cdot 10^{-3};\ \eta_b = 0{,}58\text{—}0{,}88;\ \mathrm{Re} = 0{,}02\text{—}0{,}10;\\ \mathrm{Nu}_e = 2{,}3\text{--}9{,}9;\ \mathrm{Ki}^* = 0{,}5 \div 2{,}0;\ \mathrm{Gr} = 375\text{—}180\,000.\end{gathered} \tag{20}$$

It may be supposed that Eqs. (10), (11), (15), and (17) are valid when the parameters in Eq. (20) vary over broader limits.

These conditions correspond to the case of low injection rates, since v << 3 m/sec. According to [3], the dependence u = u(v) is U-shaped in this case. With v_1, v_*, and v_2 ($v_1 < v^* < v_2$), the combustion-wave velocities are $u_1 = 0$, $|-u_*| = u_m$, $u_2 = 0$, respectively, where $u_1 = 0$ is the first "standing-wave" state and $u_2 = 0$ is the second "standing-wave" state. When $v < v_1$, collapse of the combustion occurs; when $v > v_2$ flame breakaway occurs.

NOTATION

a, c_p, μ, ρ, thermal diffusivity, specific heat, dynamic viscosity, and gravimetric density; T, temperature; g, acceleration due to gravity; $\mathrm{Pr} = \mu/c_p\lambda$, Prandtl number; $\mathrm{Gr} = \Theta L^3 g\rho/\mu^2$, Grashof number; $\Theta = 2(T^* - T_\infty)/(T^* + T_\infty)$; k_j^T, thermodiffusion coefficient; λ, thermal conductivity. Indices: T, skeleton of body; I, filtrated mixture of fuel and oxidant (injectant); ∞, value as $X \to \pm\infty$; Σ, quantities referred to the body skeleton and injectant; m, maximum; e, natural convection; j, j-th component of gas mixture; w, wall surface; *, combustion zone.

LITERATURE CITED

1. G. T. Sergeev and V. P. Pronyaev, Inzh.-Fiz. Zh., 42, No. 3, 461-466 (1982).
2. V. P. Pronyaev and G. T. Sergeev, Inzh.-Fiz. Zh., 42, No. 4, 627-633 (1982).
3. V. S. Babkin, V. I. Drobyshevich, Yu. M. Laevskii, and S. I. Potytnyakov, Fiz. Goreniya Vzryva, 19, No. 2, 17-26 (1983).
4. G. T. Sergeev, Fundamentals of Heat and Mass Transfer in Reacting Media [in Russian], Minsk (1977).
5. M. É. Aérov, O. M. Todes, and D. A. Narinskii, Apparatus with a Stationary Granular Bed [in Russian], Leningrad (1979).
6. G. T. Sergeev, Transfer Processes in Reacting and Boundary Layer, Preprint No. 23 [in Russian], A. V. Lykov Institute of Heat and Mass Transfer, Academy of Sciences of the Belorussian SSR, Minsk (1981).
7. O. N. Bryukhanov, Radiative—Convective Heat Transfer in Gas Ignition in Perforated Systems [in Russian], Leningrad (1977).

CHARACTERISTIC STATE-TRANSFORMATION TEMPERATURES OF A QUARTZ GLASS-CERAMIC WITH UNIDIRECTIONAL HEATING

G. A. Frolov, A. A. Korol', V. V. Pasichnyi,
V. Ya. Berezhetskaya, E. I. Suzdal'tsev, and
V. S. Tsyganenko

UDC 536.45

This article examines characteristic ablation temperatures of a quartz glass-ceramic. The emissivity and transparency of materials are evaluated.

Quartz glass-ceramic has been widely used in many areas of technology in recent years. The working temperatures encountered in some of these applications are significantly higher than the melting point. In particular, a device made of quartz glass-ceramic and designed to afford protection from heat at such temperatures is very effective because of the large amount of heat generated by all of the physical-chemical changes that take place during ablation. According to [1], the total heat release from glassy materials changes relatively little and may be about 11,000 kJ/kg for quartz glass. The high viscosity of melts of materials based on quartz glass makes it possible to determine the fraction of evaporation [2]. The rate of destruction of a quartz glass-ceramic is nearly independent of the amount of oxygen in the incoming gas flow, and it usually does not contain a low-temperature component (binder). All this provides grounds for the conclusion that quartz glass-ceramic is the most suitable material for studying the processes of heating and destruction during high-temperature unidirectional heating.

However, a pure quartz glass-ceramic has partial transparency, especially at temperatures above the melting point. Thus, its optical properties depend on the size of the heated volume. Moreover, a thermocouple installed in such a material will give exaggerated values of temperature due to radiative heat transfer.

Unfortunately, there is presently almost no data on absorption coefficients above the softening point not only for quartz glass-ceramic, but also for quartz glass. This makes it impossible to calculate emissivity with destruction of the surface of the material and to evaluate the error of the readings of a thermocouple inserted in a partially transparent medium.

Thus, the above-noted advantages of quartz glass-ceramic are partly offset by a serious shortcoming — its partial transparency at high temperatures.

Institute of Problems of Materials Science, Academy of Sciences of Ukrainian SSR, Kiev. Translated from Inzhenerno-Fizicheskii Zhurnal, Vol. 51, No. 6, pp. 932-940, December, 1986. Original article submitted October 16, 1985.

0022-0841/86/5106-1405$12.50